Multi-Sphere Decoding of Block Segmented SEFDM Signals with Large Number of Sub-Carriers and High Modulation Order

Tongyang Xu and Izzat Darwazeh

Department of Electronic and Electrical Engineering, University College London, London, UK
Email: t.xu@ee.ucl.ac.uk, i.darwazeh@ucl.ac.uk

***Abstract*—A non-orthogonal multicarrier signal, termed spectrally efficient frequency division multiplexing (SEFDM), is investigated in this work. It improves spectral efficiency by compressing sub-carrier spacing below the symbol rate at the cost of self-created inter carrier interference (ICI). Sphere decoding (SD) is an efficient method to recover signals approaching maximum likelihood (ML) performance. However, the complexity of the SD approaches that of ML with the increase of system size. Studies in this work show that for a small number of sub-carriers, SEFDM signals with low order modulation formats outperform spectral efficiency equivalent OFDM signals modulated by higher order modulation symbols. A key achievement is that 16QAM SEFDM signal outperforms 64QAM OFDM signal at high E_b/N_0 of the same spectral efficiency. In order to maintain the performance benefit and reduce the complexity of SD for large size SEFDM signals, multi-sphere decoding for a multi-block architecture is applied. For a large number of sub-carriers, the multi-sphere architecture works well for SEFDM signals modulated by 4QAM symbols. Whilst for 16QAM symbols, the performance is related to the number of sub-carriers. This work offers an efficient detection solution for SEFDM signals and reveals challenges. It paves the way for future study of signal detection of large size interfered multicarrier signals.**

***Index Terms*—Multicarrier communications, sphere decoding, spectral efficiency, OFDM, SEFDM, non-orthogonal.**

I. Introduction

Since the commercial deployment of 4^{th} generation (4G) long term evolution (LTE) [1] networks, research into next generation networks has been developing rapidly with significant achievements [2], [3], [4]. Although future 5^{th} generation (5G) standard (or standards) are still not fixed, one of the most important requirements is higher spectral efficiency. In the 5G research community, several groups are working to solidify the reality of 5G. There are many techniques aiming to achieve the aforementioned goal such as new waveform design [5], [6], non-orthogonal multiple access [7], massive multiple input multiple output (MIMO) [8] and millimeter wave [9]. New waveforms are capable of supporting a greater density of users, higher data rate and more efficient use of spectrum resources. There are two propositions to achieve this are; first, reducing frequency spacing between adjacent carriers; second, send data faster. Generally, both of these methods will require non-orthogonal signals, which will either compress bandwidth using spectrally efficient frequency division multiplexing (SEFDM) signals [5], [10], [11] or save time using faster than Nyquist (FTN) signals [6]. This work is focused on SEFDM signals with research ongoing since 2003 [5] with considerable effort dedicated to signal detection [12], [13], [14], [15].

978-1-5386-2123-3/17/$31.00 ©

The challenge for SEFDM is to recover signals from self-created inter carrier interference (ICI). The optimal detector is maximum likelihood (ML) where exponentially increasing complexity prohibits practical use. For the purpose of reducing complexity, a sub-optimal detector, termed sphere decoding (SD) [16], was initially proposed to decouple MIMO channels [17] and later adapted for SEFDM [12]. For small size systems, SD has a reasonable performance/complexity trade-off. For large size systems, a novel block architecture, named Block-SEFDM [18] has been designed and verified. The basic principle is to partition the entire signal band into multiple sub-bands, therefore, signal detection is simplified and distributed to multiple small sub-bands.

This work will first show the performance and complexity of single SD in condition of small number of sub-carriers and various modulation schemes. Furthermore, the work will investigate multi-SD performance and its limitations for systems with a large number of sub-carriers. Results show that for small size systems, single SD works well for SEFDM signals with various modulation schemes. However, for large size systems, the multi-SD is well suited to low order modulation schemes while is sensitive when higher order modulation formats are used due to increased interference.

II. Bandwidth Saving Model

Fundamentals of SEFDM have been comprehensively studied in [12], [13], [14], [15]. Basically, N complex symbols (e.g. M-QAM) are modulated on N non-orthogonally packed sub-carriers with a discrete expression as

$$X[k] = \frac{1}{\sqrt{Q}} \sum_{n=0}^{N-1} s_n \exp(\frac{j2\pi nk\alpha}{Q}) \quad (1)$$

where α is the bandwidth compression factor defined as $\alpha = \Delta f T$, T is the period of one SEFDM symbol and Δf denotes

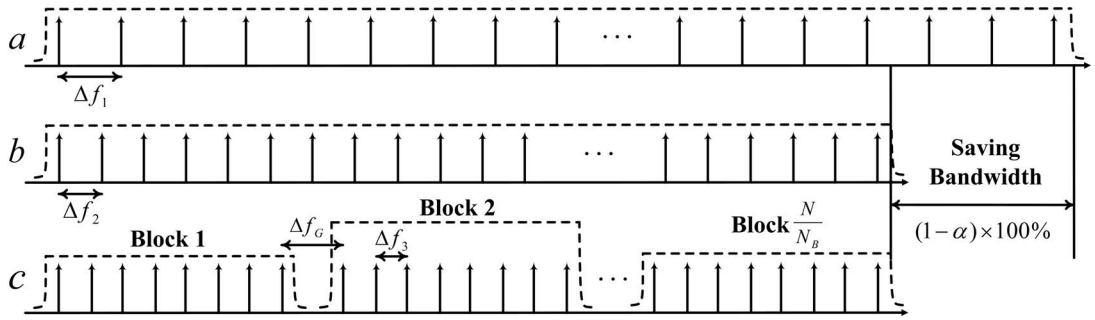

Figure 1. Spectra illustration for a) OFDM, b) SEFDM, c) Block-SEFDM. Each impulse indicates one sub-carrier and there are overall N sub-carriers for each system, respectively.

the sub-carrier spacing. $X[k]$ is the k^{th} time sample, $\frac{1}{\sqrt{Q}}$ is a scaling factor, $Q = \rho N$ and $\rho \geq 1$ is the oversampling factor. For OFDM signals $\alpha = 1$, and $\alpha < 1$ for SEFDM. The general comparison between OFDM and SEFDM is shown in Fig. 1. Fig. 1 (a) demonstrates a typical OFDM spectrum where the sub-carrier spacing Δf_1 equals $\frac{1}{T}$. Fig. 1 (b) shows a typical SEFDM system with sub-carrier spacing $\Delta f_2 = \frac{\alpha}{T}$ where $\alpha < 1$. It is apparent that the SEFDM system can save $(1-\alpha) \times 100\%$ of bandwidth compared to a typical OFDM system.

The bandwidth of OFDM and SEFDM are expressed in (2) and (3), respectively.

$$B_{OFDM} = \frac{(N-1)+2}{T} = ((N-1)+2)\Delta f \quad (2)$$

$$B_{SEFDM} = \frac{\alpha(N-1)+2}{T} = (\alpha(N-1)+2)\Delta f \quad (3)$$

With the increase of N, expressions in (2) and (3) can be simplified as

$$B_{OFDM} \approx N\Delta f \quad (4)$$

$$B_{SEFDM} \approx \alpha N\Delta f \quad (5)$$

where results indicate given a large number of N, the occupied bandwidth of SEFDM is approximately 'α' of that of the OFDM.

Furthermore, the sampled version of the signal in (1) can be simply expressed in a matrix form as:

$$X = \mathbf{F}S \quad (6)$$

where X is a Q-dimensional vector of time samples, S is an N-dimensional vector of transmitted symbols and $\mathbf{F}$ is a $Q \times N$ sub-carrier matrix with elements equal to $\exp(\frac{j2\pi nk\alpha}{Q})$ with $n = 0, 1, 2, ..., N-1$ and $k = 0, 1, 2, ..., Q-1$.

III. Inter Carrier Interference Analysis

At the receiver, X defined in (6) is contaminated by additive white Gaussian noise (AWGN) Z. The received signal is demodulated by correlating with the conjugate sub-carriers $\mathbf{F}^*$. The reception process is expressed as

$$R = \mathbf{F}^*X + \mathbf{F}^*Z = \mathbf{F}^*\mathbf{F}S + \mathbf{F}^*Z = \mathbf{C}S + Z_{\mathbf{F}^*} \quad (7)$$

where R is an N-dimensional vector of demodulated symbols, $\mathbf{C}$ is an $N \times N$ correlation matrix which is defined as $\mathbf{C} = \mathbf{F}^*\mathbf{F}$, where $\mathbf{F}^*$ denotes the $N \times Q$ conjugate sub-carrier matrix with elements equal to $e^{\frac{-j2\pi nk\alpha}{Q}}$ and $Z_{\mathbf{F}^*}$ is the AWGN correlated with the conjugate sub-carriers. Interference from non-orthogonal packed sub-carriers can be defined by using the correlation matrix $\mathbf{C}$, where elements in the matrix is expressed as

$$\mathbf{C}(m,n) = \frac{1}{Q} \times \left\{ \begin{array}{ll} Q & , \ m = n \\ \frac{1-e^{j2\pi\alpha(m-n)}}{1-e^{\frac{j2\pi\alpha(m-n)}{Q}}} & , \ m \neq n \end{array} \right\}. \quad (8)$$

In order to simplify the ICI analysis, the interference to the first sub-carrier is studied. Therefore, the first demodulated symbol $R(0)$ derived from (7) is given as

$$R(0) = \mathbf{C}(0,0)S(0) + \sum_{k=1}^{N-1} \mathbf{C}(0,k)S(k) + Z_{\mathbf{F}^*}(0) \quad (9)$$

where the first term on the right hand side indicates the desired signal and the second term is the self-created ICI component. When α=1, therefore an OFDM system, the ICI component is zero.

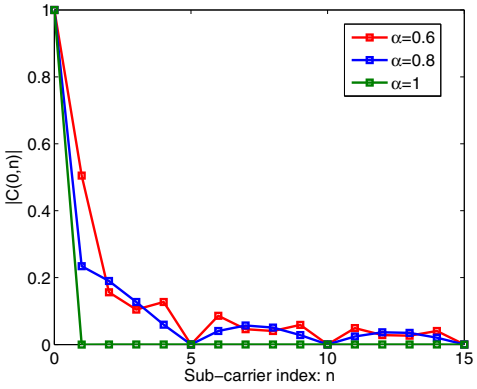

Figure 2. Desired and undesired power contributions to the first demodulated symbol $R(0)$ when N=16.

Fig. 2 shows the absolute amplitude of the desired and undesired signals. It should be noted that the desired signal

is located at n=0. In this analysis, power is normalized for desired signals. For the OFDM case, green curve shows no ICI since all the values beyond n=0 are zeros. However, it is not the case for SEFDM signals since non-zero values are evident within this range. In addition, on the second sub-carrier, the red curve (α=0.6) shows a much higher absolute value than the blue curve (α=0.8). This indicates that systems of α=0.6 would result in worse performance compared with systems of α=0.8 since interference mainly comes from adjacent sub-carriers.

The corresponding real and imaginary parts of the absolute values in Fig. 2 are presented in Fig. 3 and Fig. 4, respectively. It is shown that the interference of α=0.6 systems is mainly introduced from the imaginary part, especially the adjacent interference on the second sub-carrier.

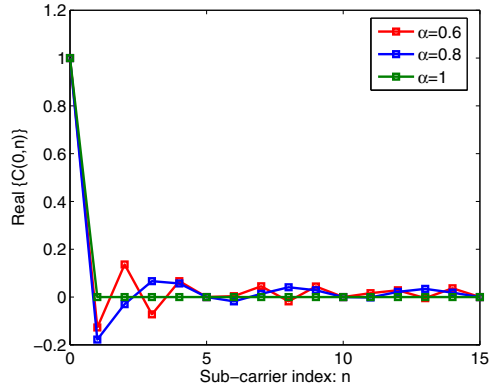

Figure 3. Real part of desired and undesired power contributions to the first demodulated symbol $R(0)$ when N=16.

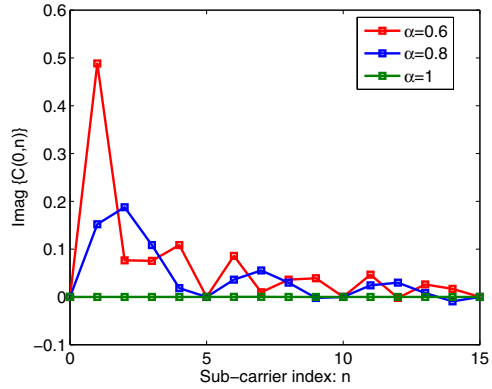

Figure 4. Imaginary part of desired and undesired power contributions to the first demodulated symbol $R(0)$ when N=16.

As explained above, the undesired ICI component is related to α. The interference contribution can be evaluated using carrier-to-interference power ratio (CIR), which is equivalent to the ratio of the desired signal power to the ICI power. Therefore, the desired signal power on the first symbol is defined as

$$P_C = |\mathbf{C}(0,0)S(0)|^2 \tag{10}$$

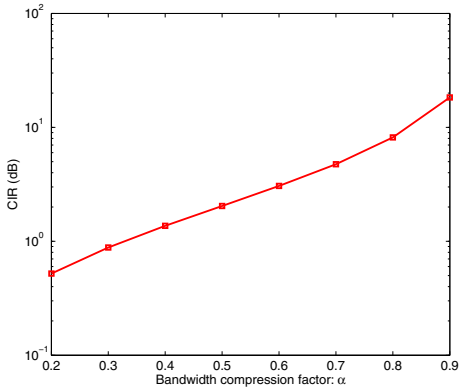

Figure 5. CIR (shown in dB) for systems at different bandwidth compression factors α when N=16.

The ICI power derived from the second term in (9) is given as

$$P_I = |\sum_{k=1}^{N-1} \mathbf{C}(0,k)S(k)|^2. \tag{11}$$

Therefore, the CIR is calculated as

$$CIR = \frac{P_C}{P_I} = \frac{|\mathbf{C}(0,0)S(0)|^2}{|\sum_{k=1}^{N-1} \mathbf{C}(0,k)S(k)|^2} = \frac{|\mathbf{C}(0,0)|^2}{|\sum_{k=1}^{N-1} \mathbf{C}(0,k)|^2} \tag{12}$$

where it is apparent that the CIR is a function of α and the numerical study of its effect is presented in Fig. 5. It is noted that the CIR is reduced with the increase of α.

IV. Block-SEFDM Descriptions

The SEFDM signal in Fig. 1 (b) is detected using a single SD detector. However, the applicability of this method is limited to systems with small number of sub-carriers. For large number of sub-carriers, a good solution is to partition a single long SD detector into multiple shorter detectors, termed multi-SD. Therefore, a new architecture, termed block-spectrally efficient frequency division multiplexing (Block-SEFDM) [18] was proposed based on the multi-SD idea. Basically, the original SEFDM spectrum in Fig. 1 (b) is separated into several blocks and a shorter SD detector can be applied in each. The spectrum partition is illustrated in Fig. 1 (c) where the entire spectrum is evenly partitioned into $\frac{N}{N_B}$ blocks where each sub-block is composed of N_B sub-carriers and every $(N_B+1)^{th}$ sub-carrier is removed. Δf_3 is the sub-carrier spacing and Δf_G is the guard band between two adjacent blocks. Due to the introduction of α, adjacent blocks are non-orthogonally packed. In addition, the guard band Δf_G reduces spectral efficiency. In order to maintain the same occupied bandwidth, sub-carriers in each block have to be packed more closer leading to a smaller Δf_3. According to Fig. 1, the

sub-carrier spacing relationship is $\Delta f_3 < \Delta f_2 < \Delta f_1$. The Block-SEFDM signal [18] is therefore expressed as

$$X[k] = \frac{1}{\sqrt{Q}} \sum_{l_B=0}^{\frac{N}{N_B}-1} \sum_{i=0}^{N_B-1} s_{i+l_B N_B} \exp[\frac{j2\pi k\beta(i+l_B(N_B+1))}{Q}] \tag{13}$$

where $s_{i+l_B N_B}$ is the i^{th} symbol modulated in the ${l_B}^{th}$ block. The product of N_B and the maximum value of l_B equals N. The in-band bandwidth compression factor (BCF) β in each block should be smaller than the effective BCF α due to the removed sub-carrier between adjacent sub-bands. The bandwidth occupations of SEFDM and Block-SEFDM are given in (14) and (15), respectively.

$$\begin{aligned} B_{SEFDM} &= \frac{\alpha(N-1)+2}{T} \\ &= (\alpha(N-1)+2)\Delta f \\ &\approx \alpha N \Delta f \end{aligned} \tag{14}$$

$$\begin{aligned} B_{Block-SEFDM} &= \frac{\beta(\frac{N}{N_B}-1+N-1)+2}{T} \\ &= (\beta(\frac{N}{N_B}-1+N-1)+2)\Delta f \\ &\approx \beta(\frac{N}{N_B}-1+N)\Delta f \end{aligned} \tag{15}$$

Therefore, according to (14) and (15), the in-band BCF β is calculated as

$$\beta = \frac{\alpha N}{\frac{N}{N_B}-1+N} \tag{16}$$

The proposed spectrum segmentation scheme provides a new way for signal detection. At the receiver, a soft demapping based iterative detection (ID) [14] algorithm is firstly executed to remove the out-of-block interference. Then, a typical SD [12] is adopted in each interference-clean block (e.g. Block 1, Block 2,...) to recover signals. The SD search for the best estimate S_{SD} in SEFDM is defined as

$$S_{SD} = \arg \min_{S \in O^N} \|R - \mathbf{C}S\|^2 \leq g \tag{17}$$

$$g = \|R - \mathbf{C}S_{ZF}\|^2 \tag{18}$$

where $\|.\|$ denotes the Euclidean norm, O is the constellation cardinality, O^N is the set of all the possible symbols combinations. g is the initial radius which equals the distance between the demodulated symbol vector R and the initial constrained estimate S_{ZF} where S_{ZF} is the zero forcing estimate which can be obtained using the rounding function $\lfloor . \rceil$ as $S_{ZF} = \lfloor \mathbf{C^{-1}}R \rceil$.

V. Bit Error Rate Performance

For small size SEFDM systems such as 16 sub-carriers, the performance of SD for different modulation schemes such as 4QAM and 16QAM is presented in Fig. 6 and Fig. 7, respectively. Results in both figures confirm that with 20% bandwidth compression (i.e. α=0.8) the performance of SEFDM approaches the same modulation scheme based OFDM one. This is consistent with the Mazo's 25% faster than the Nyquist limit [19]. In Fig. 6, for higher bandwidth saving such as 33% (i.e. α=0.67), it shows worse performance than the 4QAM OFDM one but outperforms the spectral efficiency equivalent 8QAM OFDM. It indicates that a low order modulation scheme can replace a higher one with better performance. The same benefit can be observed for 16QAM in Fig. 7 where the 16QAM SEFDM signal (α=0.8) outperforms 32QAM OFDM considering the same spectral efficiency beyond E_b/N_0=7dB. Furthermore, it is proved that the 16QAM SEFDM signal (α=0.67) even outperforms the 64QAM OFDM signal beyond E_b/N_0=11dB in Fig. 7 in the same spectral efficiency.

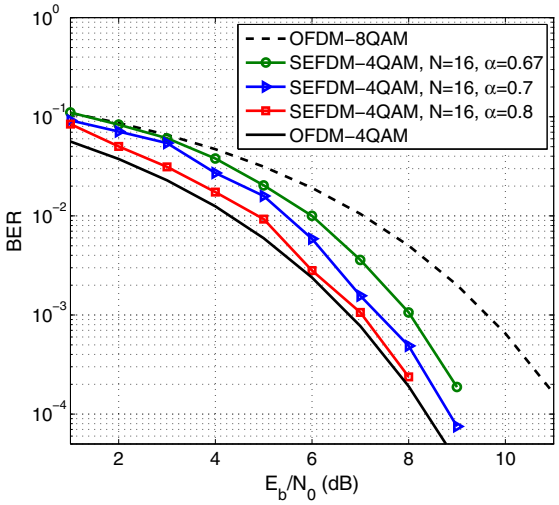

Figure 6. Single-SD results for 4QAM SEFDM with various bandwidth compression factors. 8QAM has a spectral efficiency equals to '3' and 4QAM SEFDM with α=0.67 has a spectral efficiency equals to '3'.

In practical systems, the number of sub-carriers is required to be large enough to combat multipath fading. The effective bandwidth compression factor transformation for SEFDM signals carrying 256 data sub-carriers and 16 sub-carriers in each block, is presented in Table I.

Table I
Effective Bandwidth Compression Factor Transformation
(N=256, N_B=16)

	Sub-carrier	In-band BCF	Effective BCF
$N_B = 16$	N=256	$\beta = 0.756$	$\alpha = 0.8$
		$\beta = 0.661$	$\alpha = 0.7$
		$\beta = 0.633$	$\alpha = 0.67$

The 4QAM SEFDM signals in Fig. 8 maintain the same performance benefits. However, it is not the case for the 16QAM SEFDM signals as illustrated in Fig. 9. Using 256 data sub-carriers, the performance of the 16QAM modulated SEFDM signal is no longer identical to that of the 16QAM modulated OFDM signal. The BER curve overlaps with the 32QAM result. Three reasons contribute to the reduced

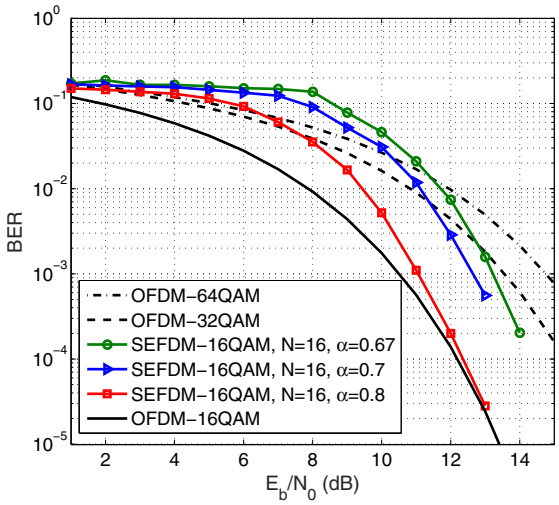

Figure 7. Single-SD results for 16QAM SEFDM with various bandwidth compression factors. 32QAM has a spectral efficiency equals to '5' and 16QAM SEFDM with α=0.8 has a spectral efficiency equals to '5'. 64QAM has a spectral efficiency equals to '6' and 16QAM SEFDM with α=0.67 has a spectral efficiency equals to '6'.

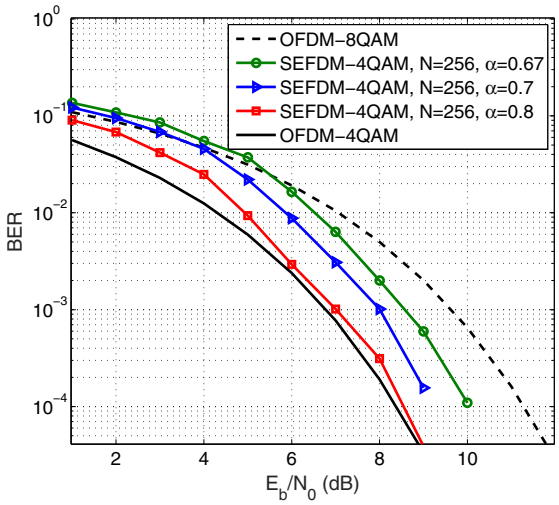

Figure 8. Multi-SD results for 4QAM symbol modulated SEFDM systems associated with different effective BCF α in the condition of N=256 and N_B=16.

performance. First, high in-band self-created ICI; Second, enhanced out-of-block interference and the last one is due to the higher density of 16QAM constellation and the decision reliability is greatly affected. One solution to mitigate the out-of-block interference is to use small number of blocks, thus small number of total sub-carriers. The in-band self-created ICI and the superimposed out-of-block interference would be reduced to some extent. The simulated performance is shown in Fig. 9 where a total number of 64 sub-carriers are used and 4 blocks are separated with each has 16 sub-carriers. The interference level, which may be indicated by in-band

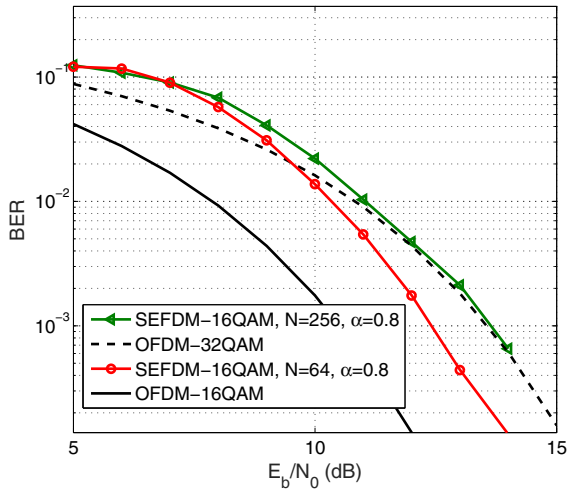

Figure 9. Multi-SD results for 16QAM symbol modulated SEFDM systems associated with different effective BCF α in the condition of N=256, 64 and N_B=16.

Table II
EFFECTIVE BANDWIDTH COMPRESSION FACTOR TRANSFORMATION
(N=64, N_B=16)

	Sub-carrier	In-band BCF	Effective BCF
$N_B = 16$	N=64	$\beta = 0.764$	$\alpha = 0.8$
		$\beta = 0.670$	$\alpha = 0.7$
		$\beta = 0.640$	$\alpha = 0.67$

bandwidth compression factor, is presented in Table II. It is clearly seen that the 20% bandwidth saving SEFDM signal outperforms the 32QAM OFDM signal by 1 dB performance gain at $BER = 10^{-3}$. However, compared with the 16QAM OFDM signal, the curve is 2 dB away.

VI. COMPLEXITY

The complexity is calculated in terms of real-valued multiplications and real-valued additions. For this we consider operations for detecting each symbol, not the operations required only once in the detection process (e.g. Cholesky Decomposition). In order to clearly show the complexity reduction of using muti-band architecture, a single SD is included for the comparison. A single SD indicates a SD detector for SEFDM signal such as shown in Fig. 1 (b). It should be noted that due to the random complexity of SD, all the nodes are assumed to be visited in this work indicating the upper bound computational expressions in (19) and (20). However, in practice, only a portion of nodes would be searched because of the search space shrink indicating a much lower computational complexity.

The upper bound computational complexity is shown in Fig. 10. For the sake of comparison, the number of operations in Fig. 10 is expressed by a logarithmic scale. The starting point of x-axis is N=16 sub-carriers and then goes up to N=256 sub-carriers. It is clearly seen that the complexity of multi-SD is substantially lower than that of the single SD. The number

of operations for both detectors increase with the value of N with the single SD detector more significant. It is noted that when N=16, they have the same complexity due to the size of each block equals 16. However, the gap becomes more obvious when the number of sub-carriers reaches 256. Based on the previous mathematical analysis in (19) and (20), it is evident that the complexity of multi-SD is proportional to the number of blocks, while in terms of the single SD, its complexity is proportional to the number of sub-carriers. Therefore, it can be inferred from the figure that the multi-band structure is suitable for large size systems while the single-band would be impractical.

$$C_{mult} = \frac{N}{N_B}(\underbrace{\sum_{n=1}^{2N_B} 2^n[2n+1]}_{full\ expansion}) \tag{19}$$

$$C_{add} = \frac{N}{N_B}(\underbrace{\sum_{n=1}^{2N_B} 2^n[2n-1]}_{full\ expansion}) \tag{20}$$

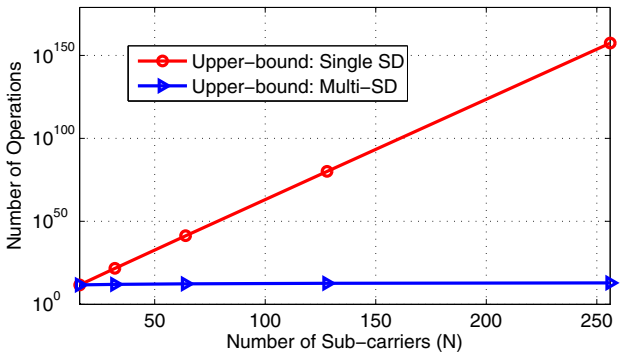

Figure 10. Upper bound of the required multiplication operations versus number of sub-carriers for two detectors.

VII. Conclusions

The performance and complexity of multi-sphere decoding for multi-block structured SEFDM signals are studied in this work. Various modulation schemes and different number of sub-carriers are investigated. The computational complexity shows significant savings of the multi-SD architecture compared to the single SD. In terms of BER performance, for small number of sub-carriers and various modulation schemes, SEFDM signals outperform OFDM singals of same spectral efficiency. A significant example is that 16QAM SEFDM signal outperforms 64QAM OFDM signal at high E_b/N_0 of equal spectral efficiency. For systems with a large number of sub-carriers, SEFDM signals modulated by 4QAM symbols still outperform spectral efficiency equivalent higher order 8QAM OFDM signals. This verifies the feasibility of the multi-sphere decoding. However, with higher order modulation formats, SEFDM systems performance is strongly compromised by the number of sub-carriers. There are multiple reasons for this with the most significant being intercarrier interference. In order to cope with this challenge, solutions such as increasing the protection guard band and pulse shaping are the subjects of ongoing work.

References

[1] 3GPP TR 36.912 v.13.0.0, "Feasibility study for further advancements for E-UTRA (LTE-Advanced)," Rel. 13, Dec. 2015.

[2] J. Andrews, S. Buzzi, W. Choi, S. Hanly, A. Lozano, A. Soong, and J. Zhang, "What will 5G be?" *Selected Areas in Communications, IEEE Journal on*, vol. 32, no. 6, pp. 1065–1082, June 2014.

[3] W. Xiang, K. Zheng, and X. Shen, *Key Enabling Technologies for 5G Mobile Communications*. Springer, 2016.

[4] F.-L. Luo and C. Zhang, *Signal Processing for 5G: Algorithms and Implementations*. Wiley, 2016.

[5] M. Rodrigues and I. Darwazeh, "A spectrally efficient frequency division multiplexing based communications system," in *Proc. 8th Int. OFDM Workshop*, Hamburg, 2003, pp. 48–49.

[6] J. Anderson, F. Rusek, and V. Öwall, "Faster-than-Nyquist signaling," *Proceedings of the IEEE*, vol. 101, no. 8, pp. 1817–1830, 2013.

[7] Y. Saito, A. Benjebbour, Y. Kishiyama, and T. Nakamura, "System-level performance evaluation of downlink non-orthogonal multiple access (NOMA)," in *Personal Indoor and Mobile Radio Communications (PIMRC), 2013 IEEE 24th International Symposium on*, Sept 2013, pp. 611–615.

[8] E. Larsson, O. Edfors, F. Tufvesson, and T. Marzetta, "Massive MIMO for next generation wireless systems," *Communications Magazine, IEEE*, vol. 52, no. 2, pp. 186–195, February 2014.

[9] T. S. Rappaport, S. Sun, R. Mayzus, H. Zhao, Y. Azar, K. Wang, G. N. Wong, J. K. Schulz, M. Samimi, and F. Gutierrez, "Millimeter wave mobile communications for 5G cellular: It will work!" *IEEE Access*, vol. 1, pp. 335–349, May 2013.

[10] T. Xu, S. Mikroulis, J. E. Mitchell, and I. Darwazeh, "Bandwidth compressed waveform for 60-GHz millimeter-wave radio over fiber experiment," *Journal of Lightwave Technology*, vol. 34, no. 14, pp. 3458–3465, July 2016.

[11] T. Xu and I. Darwazeh, "Transmission experiment of bandwidth compressed carrier aggregation in a realistic fading channel," *IEEE Transactions on Vehicular Technology*, vol. 66, no. 5, pp. 4087–4097, May 2017.

[12] I. Kanaras, A. Chorti, M. Rodrigues, and I. Darwazeh, "A fast constrained sphere decoder for ill conditioned communication systems," *Communications Letters, IEEE*, vol. 14, no. 11, pp. 999–1001, November 2010.

[13] S. Isam, I. Kanaras, and I. Darwazeh, "A truncated SVD approach for fixed complexity spectrally efficient FDM receivers," in *Wireless Communications and Networking Conference (WCNC), 2011 IEEE*, March 2011, pp. 1584–1589.

[14] T. Xu, R. C. Grammenos, F. Marvasti, and I. Darwazeh, "An improved fixed sphere decoder employing soft decision for the detection of non-orthogonal signals," *Communications Letters, IEEE*, vol. 17, no. 10, pp. 1964–1967, October 2013.

[15] T. Xu and I. Darwazeh, "A soft detector for spectrally efficient systems with non-orthogonal overlapped sub-carriers," *Communications Letters, IEEE*, vol. 18, no. 10, pp. 1847–1850, Oct 2014.

[16] B. Hassibi and H. Vikalo, "On the sphere-decoding algorithm I. expected complexity," *Signal Processing, IEEE Transactions on*, vol. 53, no. 8, pp. 2806–2818, Aug 2005.

[17] A. Burg, M. Borgmann, M. Wenk, M. Zellweger, W. Fichtner, and H. Bolcskei, "VLSI implementation of MIMO detection using the sphere decoding algorithm," *Solid-State Circuits, IEEE Journal of*, vol. 40, no. 7, pp. 1566–1577, July 2005.

[18] T. Xu and I. Darwazeh, "Multi-Band reduced complexity spectrally efficient FDM systems," in *9th IEEE/IET International Symposium on Communication Systems, Networks & Digital Signal Processing 2014 (CSNDSP14)*, Manchester, United Kingdom, Jul. 2014, pp. 904–909.

[19] J. Mazo, "Faster-than-Nyquist signaling," *Bell Syst. Tech. J*, vol. 54, no. 8, pp. 1451–1462, 1975.